cancers

MDPI

Communication

Gold Glyconanoparticles Combined with 91–99 Peptide of the Bacterial Toxin, Listeriolysin O, Are Efficient Immunotherapies in Experimental Bladder Tumors

Hector Terán-Navarro [1,†], Andrea Zeoli [1,†], David Salines-Cuevas [1], Marco Marradi [2], Noemi Montoya [3], Elena Gonzalez-Lopez [4], Javier Gonzalo Ocejo-Vinyals [4], Mario Dominguez-Esteban [5], Jose Luis Gutierrez-Baños [5], Felix Campos-Juanatey [5], Sonsoles Yañez-Diaz [1,6], Almudena Garcia-Castaño [7], Fernando Rivera [7], Ignacio Duran [7] and Carmen Alvarez-Dominguez [1,3,*]

1 Grupo de Oncología y Nanovacunas, Instituto de Investigación Marqués de Valdecilla (IDIVAL), 39011 Santander, Cantabria, Spain; hteran35@hotmail.com (H.T.-N.); andrea.zeoli@libero.it (A.Z.); davidsalcines@gmail.com (D.S.-C.); sonsolesjuana.yanez@scsalud.es (S.Y.-D.)
2 Dipartimento di Chimica "Ugo Schiff", Universitá Degli Studi di Firenze, I-50019 Firenze, Italy; marco.marradi@unifi.it
3 Grupo de Investigación MEDONLINE, Facultad de Ciencias de la Salud, Universidad Internacional de La Rioja, Avda. de La Paz 137, 26006 Logroño, La Rioja, Spain; noemi.montoya@unir.net
4 Servicio de Inmunología, Hospital Universitario Marqués de Valdecilla, Instituto de Investigación Marqués de Valdecilla (IDIVAL), 39008 Santander, Cantabria, Spain; elena.gonzalez@scsalud.es (E.G.-L.); javiergonzalo.ocejo@scsalud.es (J.G.O.-V.)
5 Servicio de Urología, Hospital Universitario Marqués de Valdecilla, Instituto de Investigación Marqués de Valdecilla (IDIVAL), 39008 Santander, Cantabria, Spain; mario.dominguez@scsalud.es (M.D.-E.); joseluis.gutierrez@scsalud.es (J.L.G.-B.); felix.campos@scsalud.es (F.C.-J.)
6 Servicio de Dermatología, Hospital Universitario Marqués de Valdecilla, Instituto de Investigación Marqués de Valdecilla (IDIVAL), 39008 Santander, Cantabria, Spain
7 Servicio de Oncología Médica, Hospital Universitario Marqués de Valdecilla, Instituto de Investigación Marqués de Valdecilla (IDIVAL), 39008 Santander, Cantabria, Spain; almudena.garcia@scsalud.es (A.G.-C.); fernando.rivera@scsalud.es (F.R.); ignaciojose.duran@scsalud.es (I.D.)
* Correspondence: carmen.alvarezd@scsalud.es; Tel.: +34-687492768
† These authors contribute equally to this work.

Simple Summary: We propose a novel type of immunotherapy for bladder cancer using gold nanoparticles bound to a peptide of a bacterial toxin with anti-tumor capacities as listeriolysin O called Listeria nanovaccines. Here, we present the pre-clinical experiments on a mice model of bladder cancer and blood cells of patients with bladder cancer using these Listeria nanovaccines that activate the immune system, block the tumor immunosuppression environment, and reduce the tumor size. The impact of Listeria nanovaccines on the field of immunotherapies for solid tumors can be extended to other solid tumors containing lymphocyte infiltration. Therefore, we propose Listeria nanovaccines as immunotherapy for tumors such as melanoma, urothelial bladder carcinoma, non-small cell lung carcinoma, and glioblastoma.

Abstract: This study presents proof of concept assays to validate gold nanoparticles loaded with the bacterial peptide 91–99 of the listeriolysin O toxin (GNP-LLO$_{91–99}$ nanovaccines) as immunotherapy for bladder tumors. GNP-LLO$_{91–99}$ nanovaccines showed adjuvant abilities as they induce maturation and activation of monocyte-derived dendritic cells (MoDCs) to functional antigen-presenting cells in healthy donors and patients with melanoma or bladder cancer (BC), promoting a Th1 cytokine pattern. GNP-LLO$_{91–99}$ nanovaccines were also efficient dendritic cell inducers of immunogenic tumor death using different bladder and melanoma tumor cell lines. The establishment of a pre-clinical mice model of subcutaneous BC confirmed that a single dose of GNP-LLO$_{91–99}$ nanovaccines reduced tumor burden 4.7-fold and stimulated systemic Th1-type immune responses. Proof of concept assays validated GNP-LLO$_{91–99}$ nanovaccines as immunotherapy by comparison to anti-CTLA-4 or anti-PD-1 antibodies. In fact, GNP-LLO$_{91–99}$ nanovaccines increased percentages of CD4$^+$ and CD8$^+$ T cells, B cells, and functional antigen-presenting DCs in tumor-infiltrated lymphocytes, while they reduced

check for updates

Citation: Terán-Navarro, H.; Zeoli, A.; Salines-Cuevas, D.; Marradi, M.; Montoya, N.; Gonzalez-Lopez, E.; Ocejo-Vinyals, J.G.; Dominguez-Esteban, M.; Gutierrez-Baños, J.L.; Campos-Juanatey, F.; et al. Gold Glyconanoparticles Combined with 91–99 Peptide of the Bacterial Toxin, Listeriolysin O, Are Efficient Immunotherapies in Experimental Bladder Tumors. *Cancers* **2022**, *14*, 2413. https://doi.org/10.3390/cancers14102413

Received: 10 March 2022
Accepted: 6 May 2022
Published: 13 May 2022

the levels of myeloid-derived suppressor cells (MDSC) and suppressor T cells (T_{reg}). We conclude that GNP-$LLO_{91–99}$ nanovaccines can work as monotherapies or combinatory immunotherapies with anti-CTLA-4 or anti-PD-1 antibodies for solid tumors with high T cell infiltration, such as bladder cancer or melanoma.

Keywords: listeriolysin O; melanoma; bladder cancer; nanoparticles; immunotherapy

1. Introduction

In the past 10 years, nanotechnology has been widely studied for cancer treatment, as nanoparticles can play a significant role in drug delivery systems [1]. In this regard, inorganic nanoparticles such as gold nanoparticles (AuNP) are useful candidates since the gold core is inert and non-toxic and can be surface-functionalized with different compounds. Functionalization with carbohydrates might enhance their accumulation into tumors and overcome drug resistance. In addition, the AuNP combination with peptides might target them to specific cells or confer novel features [2,3]. In this regard, gold glyconanoparticles (AuGNP)—here, GNP for simplicity—present several advances such as high water solubility, ability to target antigen-presenting cells (APC), lack of toxicity [4,5], and capacity to combine in the same design with different ligands, such as carbohydrates and peptides [6,7].

Adjuvants are classical immunotherapies that activate the tumoral immune responses by acting on antigen-presenting cells (APCs) (e.g., dendritic cells, DCs); examples are inorganic nanoparticles, cancer vaccines, oligonucleotides, bacterial compounds, and antagonists of Toll-like receptors [8,9]. However, the development of immune checkpoint inhibitors (ICIs) (e.g., anti-CTLA-4 or anti-PD-1/PD-L1 antibodies) as new immunotherapies changed the focus of immune system activation to T cells, as they block the negative immune controls of T cells and boost the anti-tumoral immune responses [10]. ICIs have been approved as either a neoadjuvant or first-line treatment for tumors such as melanoma, non-small cell lung (NSCLC), renal, or bladder cancer (BC). In general, ICIs seem to benefit oncologic patients with tumors presenting high T cell infiltration and mutational variance. However, in some cases, ICI resistance or adverse effects minimize their efficiency [11], along with the failure to respond to ICI of tumors with low-medium mutational variance (e.g., hepatocarcinoma) or infiltrated T cells (e.g., glioblastoma) [12–16].

Bladder cancer (BC) is the ninth most common malignancy diagnosed worldwide. As a tumor, BC is highly immunogenic and T cell-infiltrated. It has been postulated that a dysregulation of the immune system within the bladder promotes BC growth. However, to date, this immunosuppression within BC has not been characterized in detail [17]. BC arises from the urothelium, the epithelium that lines the urinary bladder, and only 25% at most are muscle-invasive metastatic BCs. Metastatic BC is treated with chemotherapy regimens as first-line treatments and, recently, ICI as neoadjuvant, maintenance or second-line treatment [18]. Most BCs are superficial, low-grade, noninvasive, or superficial tumors confined to the mucosa layer. Noninvasive BC standard therapy implies tumor resection followed by adjuvant therapy with the bacterium Bacillus Calmette-Guerin (BCG) to activate the immune system [19,20]. In this regard, *Listeria monocytogenes* is a human bacterial pathogen also used for the treatment of several tumors such as prostate cancer, cervix carcinoma, or pancreatic cancer, using attenuated mutants that lack the C-terminal domain of the main virulence factor, listeriolysin O (LLO) [21–23]. Moreover, LLO is a pore-forming toxin that, along with its cytolytic activity, induces cell death of different cell types such as DCs, macrophages, or T cells [24]. LLO seems to induce different types of cell death, necrosis, necroptosis, pyroptosis, or apoptosis, causing different effects [25]. The classical assumption that necrosis induces inflammatory immune responses while apoptosis triggers anti-inflammatory immune responses does not seem applicable in all contexts of cell death by bacterial toxins. While the tuberculosis-necrotizing toxin (TNT) induces

immunological silent cell death that recruits macrophages and induces poor immune responses [26], LLO action onto tumor cells appears to induce an immunogenic cell death characterized by promoting inflammatory and anti-tumor immune responses. Previous work of our group quoted LLO anti-neoplastic abilities to 91–99 N-terminal peptides and explored different vaccine vectors as therapy for experimental melanoma [5–7]. Here, we extend these studies using a nanocarrier vector GNP coupled to two ligands, the 91–99 LLO peptide and β-D-glucose (here called GNP-$LLO_{91–99}$ nanovaccines), to validate them as valid immunotherapies for bladder tumors and inducers of immunogenic apoptosis.

2. Materials and Methods

2.1. Cells and Mice

B16.F10 murine metastatic melanoma, A375 human melanoma, MB-49 murine and human T-24 bladder tumor cell lines, TC-1 murine and A-549 NSCLC lung tumor cell lines, O627 murine glioblastoma cell lines, Hepa1-6 murine hepatocarcinoma cell lines, CHO hamster ovary cell lines and SV-40-induced IC-21 murine macrophage cell lines were obtained from ATCC (Manassas, VA, USA). The RG-1 human glioblastoma cell line was a gift of J. L. Fernandez-Luna (HUMV, Santander, Spain). C57BL/6 male or female mice (Charles River, L'Abresle, France) 8–12 months of age were used in the study.

2.2. Patients

Nine patients with advanced solid tumors were included in this study: three patients with stage IV melanoma before enrollment in immunotherapy (MEL-1 and MEL-3), a stage IIIB cutaneous melanoma after surgery resection (MEL-2), a lung and bladder carcinoma treated with cisplatin-etoposide (BC-1), two urothelial bladder carcinomas without treatment (BC-2, BC-3), a hepatocellular carcinoma treated with ablation by microwaves (HEP-1), a prostate adenocarcinoma treated with taxocel (PROST-1), and a multiform glioblastoma treated with temozolomide and radiotherapy (GLIO-1). MEL-1, MEL-3, BC-1, HEP-1, PROST-1, and GLIO-1 were diagnosed at the Medical Oncology Department; BC-2 and BC-3 were diagnosed at the Urology Department; and MEL-2, the stage IIIB cutaneous melanoma, was diagnosed at the Dermatology Department (Hospital U. Marqués de Valdecilla, HUMV, Santander, Spain). The patients participated in the study voluntarily, signed an informed consent agreement at the physician consultation, and received an information document on the research study. Patients were able to revoke the informed consent at any time. Healthy donors were obtained from the blood bank at our hospital. Blood samples were obtained in heparin tubes at the Dermatology, Urology, or Medical Oncology Departments on the day of patient consultation and processed at the IDIVAL laboratory within the following 2 h.

2.3. Preparation of GNP-$LLO_{91–99}$ Nanovaccines

$LLO_{91–99}$ peptide with a C-terminal cysteamide ($LLO_{91–99}C(O)NHCH_2CH_2SH$, 14 mg, purity 95%) was purchased from GenScript (Piscataway, NJ, USA) and 5-(mercapto)pentyl-β-D-glucopyranoside ($GlcC_5SH$) was prepared as reported previously by our group [27]. GNPs carrying 90% glucose and 10% $LLO_{91–99}$ peptide were prepared by the reduction of Au(III) salt with sodium borohydride following previously described procedures [28]. Peptide loading was GNP-$LLO_{91–99}$: 8.9 μg ($LLO_{91–99}$)/0.182 mg of GNPs. In brief, $LLO_{91–99}C(O)NHCH_2CH_2SH$ (1 mg, 0.85 μmol) and $GlcC_5SH$ (2.1 mg, 7.4 μmol) were dissolved in deuterated water (750 μL). ^1H NMR analysis of the mixture showed a Glc:$LLO_{91–99}$ ratio of ~9:1 (e.g., 90% Glc and 10% $LLO_{91–99}$). The above-prepared solution of the ligands (0.011 M, 4 equivalents) was added with an aqueous solution of $HAuCl_4$ (100 μL, 0.025 M, 1 equivalent), followed by an aqueous $NaBH_4$ solution (67.5 μL, 1 M, 27 equivalents) in four portions under rapid shaking. The dark dispersion was shaken for 2 h and then filtered with 3 KDa MWCO tubes by centrifugal filtering. The black colloid was recovered with water and lyophilized (0.482 mg). The residue was re-dispersed in the minimum volume of water, loaded in SnakeSkin pleated dialysis tubing (Pierce,

10 KDa MWCO), and dialyzed against 3 L of water under gentle stirring, recharging with fresh distilled water every ~8 h over the course of 72 h. After lyophilization, 0.456 mg of GNP-LLO$_{91–99}$ were obtained. The ratio of glucose/peptide in the GNP was determined by quantitative NMR (qNMR) in a Bruker AVANCE 500 MHz spectrometer: 0.456 mg of GNP-LLO$_{91–99}$ was dispersed in D_2O 99.9% (200 µL). Then, 80 µL of this solution was added to 40 µL of a 0.05% 3-(trimethylsilyl)propionic-2,2,3,3-d_4 acid sodium salt (TSP-d4) solution in D_2O and 60 µL of D_2O. ^{1}H NMR analysis of the mixture allowed the calculation of the amount of peptide in the GNP-LLO$_{91–99}$: 8.9 µg (LLO$_{91–99}$)/0.182 mg (GNP). TEM (JEOL JEM-2100F working at 200 kV). A single drop (5 µL) of the aqueous dispersion (ca. 0.1 mg mL^{-1} in MilliQ water) of the GNPs was placed onto a copper grid coated with an ultrathin carbon film (Electron Microscopy Sciences). The grid was air-dried for 12 h at RT. Average gold diameter was 1.5 ± 0.5 nm, obtained by counting 600 particles in the TEM image as previously reported [28]. UV/Vis (Beckman Coulter DU 800 Spectrometer, H_2O, 0.1 mg/mL): The average gold core size was confirmed by UV-Vis spectra, which did not show an absorption maximum at around 520 nm, typical of gold nanoparticles with a larger core diameter [29].

2.4. Isolation of MoDCs from Healthy Donors and Patients and Preparation of Murine DCs

Leukocytes from whole blood cells were collected from the interphase of a Ficoll gradient and incubated with microbeads conjugated to a mouse IgG2a monoclonal anti-CD14 antibody and passed through MACS^{TM} columns (Miltenyi, Bergisch Gladbach, Germany) to select monocytes (Mo) as CD14$^+$ positive cells. Mo (1×10^6 of cells/mL) were cultured in 6-well plates (Falcon^{TM}, Corning Life Sciences, Glendale, AZ, USA) over 7 days using GM-CSF (50 ng/mL) and IL-4 (20 ng/mL) in RPMI-20% FCS medium. Differentiated MoDCs were 98% CD45$^+$CD11c$^+$HLA-DR$^{+/-}$CD86$^-$CD14$^-$ positive cells. Bone-marrow-derived dendritic cells (here called DC) were obtained from C57BL/6 control or bladder-transplanted mice femurs and differentiated with GM-CSF (20 ng/mL) for 7 days. Differentiated DCs presented a phenotype of 98% CD11c$^+$MHC-I$^+$MHC-II$^+$CD11b$^{-/+}$CD40$^-$CD86$^-$ cells.

2.5. Direct and Immunogenic Apoptosis of Melanoma and Bladder Tumor Cells

Cell toxicity was first evaluated using Trypan blue staining and incubation for 16 h with GNP-LLO$_{91–99}$ nanovaccines. Direct apoptosis was evaluated in the different tumor cell lines after incubation for 16 h with GNP-LLO$_{91–99}$ (50 µg/mL). Immunogenic apoptosis implies the incubation of tumor cell lines with $\frac{1}{2}$ supernatants of ex vivo differentiated DCs (for murine tumors) or MoDCs from healthy donors (for human tumors), pre-treated for 16 h with 50 µg/mL of GNP-LLO$_{91–99}$ nanovaccines. Direct and immunogenic apoptosis was examined by FACS after double staining with the DNA marker, 7-AAD (7-AAD-PE), and the apoptotic marker, annexin V (annexin V-APC). The staining of cells with 7-ADD corresponded to necrotic cell death, whereas the staining of cells with annexin-V alone corresponded to early apoptotic programmed cell death (mean ± SD). Experiments involving human samples were performed three times and five times for mice assays. Results are expressed as the % of apoptotic cells ± SD of triplicate samples ($p \leq 0.5$).

2.6. Bladder Tumor Auto Transplants Followed by GNP-LLO$_{91–99}$ and ICI Immunotherapies

Murine MB-49 bladder cell lines [27] or B16.F10 melanoma were transplanted into 8–12-week-old C57BL/6 male or female mice (auto transplants), respectively, with a single subcutaneous (s.c.) injection (10^6 cells) in a volume of 100 µL (n = 10/group). At 14 days, tumor transplanted mice received or not (NT) a single intravenous (i.v.) inoculation of GNP-LLO$_{91–99}$ nanovaccines (50 µg/mouse). On day 7, mice were sacrificed, and tumor sizes were measured with a caliper. Values shown for tumor volume (TV) were calculated using the following formula: (length × (width)^2)/2, as reported [6]. Mean and SD of the tumor volumes per group were calculated. Sera were also obtained, processed, and used for cytokine measurements. Tumors were minced, homogenized, passed through a 70 µm

strainer, and then centrifuged over a Ficoll gradient at a 1.077 g/mL density (Histopaque-1077, Sigma-Aldrich, St. Louis, MO, USA) to recover TILs in the interphase gradient while collecting tumor cells in pellets. For immunotherapeutic studies, treatment of MB-49 established transplants with GNP-LLO$_{91–99}$ nanovaccines were performed as above, alone or in combination with the following antibodies: anti-CTLA-4 or anti-PD-1 (50 µg/mouse). Cell populations of TILs and spleens were analyzed by FACS. All experiments were performed at least five times.

2.7. FACS Analysis and Cytokines

Cell surface markers of human MoDCs were analyzed by FACS using the following antibodies for human MoDC: anti-HLA-DR-FITC, anti-CD45-PerCP, anti-CD11c-APC, anti-CD14-PE, and anti-CD86-V450 (clone 2331). Murine spleens and TILs were analyzed by FACS using the following antibodies: biotin anti-IAb (clone AF6-120-1), anti-CD11c-PE (clone HL3), anti-CD40-APC (monoclonal 3/23 from BD Pharmingen, BD Biosciences, San Jose, CA, USA), anti-CD86-V450 (clone GL-1), anti-CD4-FITC (clone RPA-T4), and anti-CD8-PE (clone RPA-T8, BD Biosciences, San Jose, CA, USA). All the samples were treated with propidium iodide to gate dead cells. Flow cytometry was performed with a FACSCalibur (BD Biosciences, San Jose, CA, USA). Cytokines in mice sera, DC, or MoDC supernatants were quantified using multiparametric Luminex kits. In brief, IFN-gamma, IL-2, IL-4, IL-6, IL-10, IL-12 (p70), IL-17A, KC/CXCL1, MIP-2, and TNF-α levels in mice serum samples were quantified using the Luminex 200 platform with a magnetic system (Milliplex MAP Mouse High Sensitivity T Cell Magnetic Bead Panel, EMD Millipore Corporation, Billerica, MA, USA) following the manufacturer's instructions. Cytokine concentrations are expressed as the averages of three replicates in pg/mL ± SD. Human cytokines in MoDC supernatants were quantified using the multiparametric Luminex kit (Milliplex human HSTCMAG-28SK including the following cytokines: IFN-γ, IL-10, IL-17A, IL-2, IL-4, IL-6, and TNF-α; EMD Millipore Corporation, Billerica, MA, USA) following the manufacturer's instructions.

2.8. Statistical Analysis

For statistical analysis, Student's *t*-test was applied to mice with auto transplants; each group included 5 mice for all assays reported ($p \leq 0.05$ was considered significant). Experiments in mice were performed at least five times each, and experiments with MoDCs from healthy donors or oncologic patients and tumor cell lines were performed three times each. ANOVA analysis was applied to cytokine measurements and flow cytometry analysis per the manufacturer´s recommendations ($p \leq 0.05$ was considered significant). For statistical purposes, each flow cytometry sample was performed in triplicate. The GraphPad software was used for the generation of all the graphs presented.

3. Results and Discussion

We initiated this study with the hypothesis that GNP-LLO$_{91–99}$ nanovaccines might function as immunotherapies for bladder tumors and planned the following assays: adjuvant abilities using MoDCs from human donors, the in vitro immunogenic death of murine and human tumor cell lines, the in vivo anti-neoplastic action after the establishment of a mouse bladder cancer model, and immunotherapeutic actions in comparison to anti-CTLA-4 or anti-PD-1 immunotherapies.

3.1. GNP-LLO$_{91–99}$ Nanovaccines Showed No Toxicity in Human MoDCs or Mice

Before initiating any experiment, we prepared a homogeneous batch of GNP-LLO$_{91–99}$ nanovaccines to be used in all the experiments and performed the quality and toxicity controls in vivo and in vitro. GNP-LLO$_{91–99}$ nanovaccines are formed by a gold core covalently linked to LLO$_{91–99}$ peptide and β-D glucose (GNP-LLO$_{91–99}$ nanovaccines schematic representation in Figure 1a). The gold core had a spheric shape and nanometric size with an average of 2 nm, as observed by the analysis of transmission electron microscopy

(Figure 1b). Different concentrations of GNP-LLO$_{91–99}$ nanovaccines or LLO$_{91–99}$ peptide (5–500 µM) were non-toxic for human MoDCs after incubation for 16 h, as determined by evaluating the cell viability with Trypan blue staining (Figure 1c). We also observed no toxicity in mice (C52BL/6 male and female, n = 10) when we inoculated intraperitoneally (i.p.) for 16 h with GNP-LLO$_{91–99}$ nanovaccines or LLO$_{91–99}$ peptide (5–500 µM) (Figure 1c, center and right columns) and examined mice health conditions and sera IL-1 concentrations.

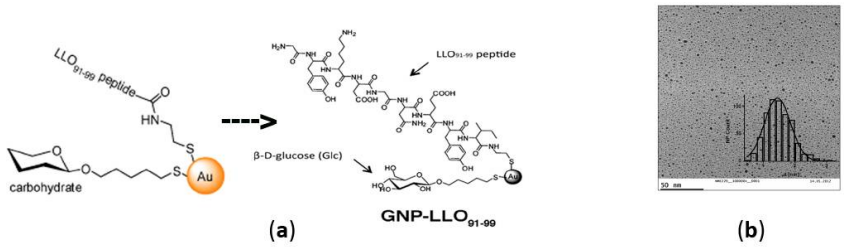

(**a**) (**b**)

Reagent	*In vitro toxicity* (DC)	*In vivo* toxicity (C57BL/6 mice)	
		Health condition	IL-1 (pg/mL)
NI	1.80 x 10^6 ± 102	Normal	11 ± 0.1
LLO$_{91-99}$ (µM)			
500	1.29 x 10^6 ± 140	Normal	16 ± 0.2
50	1.83 x 10^6 ± 122	Normal	11 ± 0.1
5	1.81 x 10^6 ± 113	Normal	12 ± 0.2
GNP-LLO$_{91-99}$ (µM)			
500	1.30 x 10^6 ± 133	Normal	17 ± 0.2
50	1.82 x 10^6 ± 131	Normal	12 ± 0.2
5	1.82 x 10^6 ± 103	Normal	11 ± 0.2
Anti-CTLA-4 (µM)			
500	0.88 x 10^6 ± 101	Sick*	
50	1.79 x 10^6 ± 102	Normal	
5	1.80 x 10^6 ± 103	Normal	
Anti-PD-1 (µM)			
500		Normal	
50		Normal	
5		Normal	

(**c**)

Figure 1. Preparation of GNP-LLO$_{91–99}$ nanovaccines, quality, and toxicity controls in vitro and in vivo. (**a**) Schematic representations of GNP-LLO$_{91–99}$ nanovaccines and chemical structure showing localization of LLO$_{91–99}$ peptide and the carbohydrate, β-D-glucose. (**b**) Transmission electron microscopy (TEM) image (100,000×), including the size histogram that shows the spherical shape and nanometric size of the gold core of GNP-LLO$_{91–99}$. (**c**) In vitro toxicities of GNP-LLO$_{91–99}$ nanovaccines were explored in MoDCs of healthy donors incubated for 16 h with different concentrations of GNP-LLO$_{91–99}$ nanovaccines or LLO peptide, LLO$_{91–99}$ (5–500 µM) to examine cell viability with Trypan-blue staining. Results are expressed as the mean of viable cells ± SD. For in vivo analyses, we inoculated mice (12 months old male, n = 5, or female, n = 5) intravascularly (i.v.) with the same concentrations of GNP-LLO$_{91–99}$ nanovaccines and LLO$_{91–99}$ peptide as in (**a**) (5–500 µM) in C57BL/6 mice for 16 h, examined mice health conditions, and measured IL-1 concentration in mice sera. Experiments were performed five times each. Results are expressed as the mean cytokine concentrations (pg/mL) ± SD. * Sick, refers to animals with hairless and difficulties to move and feed.

3.2. GNP-LLO$_{91–99}$ Nanovaccines Served as Adjuvants for Human MoDCs of Oncologic Patients

Once we established that GNP-LLO$_{91–99}$ nanovaccines showed no toxicity in human MoDC, we next explored their abilities as adjuvants. Functional and activated MoDCs are characterized by three molecules relevant to combat tumors, the surface expression of MHC-I and MHC-II molecules necessary for antigen presentation, and CD86 co-stimulatory molecules essential for T cell activation. MoDC cytokine production is also a determinant of T cell activation or suppression. In this regard, MoDC activation corresponds with a high production of Th1 cytokines, such as IL-12p70, which stimulates cytotoxic T cells, or TNF-a, which implements innate immunity. Meanwhile, suppression is induced by classical Th2 cytokines, such as IL-6 or IL-10, which promote significant numbers of T_{reg} [19] as well as KC or MIP-2 chemokines that also participate, as they can trigger the migration of MDSC.

The ability of an adjuvant to induce both maturation and activation of ex vivo cultured DCs requires an optimal and basal functionality of these cells [30], which is not always observed in cancer patients, as reported in hepatocarcinoma or multiple myeloma [12,13,31,32]. For this reason, we evaluated GNP-LLO$_{91–99}$ nanovaccines as adjuvants after the ex vivo incubation of MoDCs from healthy donors or patients with melanoma (MEL-1, MEL-2) or bladder carcinoma (BC-1, BC-2) from our institution (Hospital U. Marqués de Valdecilla, HUMV, Santander, Spain) (Supplementary Table S1). GNP-LLO$_{91–99}$ nanovaccines showed three-fold increases in the percentages of MHC-I or MHC-II and five-fold increases in the co-stimulatory CD86 molecules after incubation of MoDCs in healthy donors (CONT), patients with melanoma (MEL-1, MEL-2), lung and bladder tumors (BC-1), or urothelial bladder tumors (BC-2) (GNP-LLO$_{91–99}$ bars in Figure 2a). Empty GNP nanovaccines or LLO$_{91–99}$ peptides (data not shown) had no effect on the surface expression of MHC-I, MHC-II, or CD86 molecules, similar to MoDCs treated with saline (CONT + GNP and CONT bars in Figure 2a), as reported previously [7].

Analysis of Th1 and Th2 cytokines indicated that GNP-LLO$_{91–99}$ nanovaccines increased the production of Th1 cytokines in MoDCs of healthy donors, especially TFN-α and IL-12p70 (CONT versus CONT + GNP-LLO$_{91–99}$ rows in Table 1). Empty GNP nanovaccines showed similar patterns as saline-treated MoDCs (CONT versus CONT + GNP rows in Table 1), indicating that empty GNP showed no adjuvant effect.

Table 1. Production of cytokines by MoDCs stimulated or not with GNP-LLO$_{91–99}$ nanovaccines.

Patient Code	Clinical Symptoms and Treatment [a]	IL-12 [b,*]	IL-6	IL-10	TNF-α
MEL-1	Metastatic melanoma (IV) NT	0.3 ± 0.1	6.4 ± 0.9	5.6± 0.9	6.25 ± 0.1
MEL-1 + GNP-LLO$_{91–99}$	Metastatic melanoma (IV) NT	4.7 ± 0.1	2.22 ± 0.2	1.61 ± 0.1	66 ± 1.3
MEL-2	Nodular melanoma (IIIB) surgery	0.5 ± 0.1	6.1 ± 0.1	6.6 ± 0.1	8.78 ± 0.1
MEL-2 + GNP-LLO$_{91–99}$	Nodular melanoma (IIIB) surgery	6.5 ± 0.2	2.07 ± 0.1	1.7 ± 0.1	50 ± 1.2
BC-1	Lung–bladder carcinoma Cisplatin–etoposide	0.2 ± 0.1	6.0 ± 0.1	4.6 ± 0.1	7.8 ± 0.1
BC-1 + GNP-LLO$_{91–99}$	Lung–bladder carcinoma Cisplatin–etoposide	6.4 ± 0.1	2.3 ± 0.1	1.2 ± 0.1	220 ± 1.4
BC-2	Urothelial bladder carcinoma NT	0.3 ± 0.2	7.1 ± 0.2	5.1 ± 0.2	8.1 ± 0.1
BC-2 + GNP-LLO$_{91–99}$	Urothelial bladder carcinoma NT	7.2 ± 0.3	2.1 ± 0.1	0.9 ± 0.2	204 ± 1.6
CONT	NONE	0.8 ± 0.1	3.1 ± 0.1	2.4 ± 0.1	2.0 ± 0.1
CONT + GNP	NONE	0.7 ± 0.1	2.8 ± 0.1	2.3 ± 0.1	1.8 ± 0.1
CONT + GNP-LLO$_{91–99}$	NONE	6.0 ± 0.2	4.1 ± 0.2	3.5 ± 0.1	150 ± 0.2

[a] Clinical symptoms and treatments of patients with informed consent selected for the study. CONT, healthy donors. [b] Cytokines are measured in sera of patients (Luminex kits, EMD Millipore Corporation, Billerica, MA, USA). Results are the mean of cytokine concentrations (pg/mL) ± SD (* $p \leq 0.05$).

MoDCs from patients with melanoma or lung and bladder carcinoma showed under non-stimulated conditions a clear Th2 cytokine pattern (e.g., IL-6 and IL-10, high levels) that reflects the systemic cytokine pattern of the patient's sera (Supplementary Table S1). Incubation of MoDCs with GNP-LLO$_{91–99}$ nanovaccines shifted Th2 to Th1. In fact, we detected high levels of IL-12p70 and reduced levels of IL-10 (MEL-1-GNP-LLO$_{91–99}$, MEL-2-GNP-LLO$_{91–99}$, BC-1-GNP-LLO$_{91–99}$, and BC-2-GNP-LLO$_{91–99}$ rows in Table 1). Therefore, GNP-LLO$_{91–99}$ nanovaccines seem to be valid adjuvants for patients with melanoma or BC

but also for MoDCs of patients with other tumors (e.g., prostate adenocarcinoma, NSCLC lung cancer, or glioblastoma), except for those reported with a low DC functionality such as hepatocellular carcinoma [13] (Supplementary Figure S1).

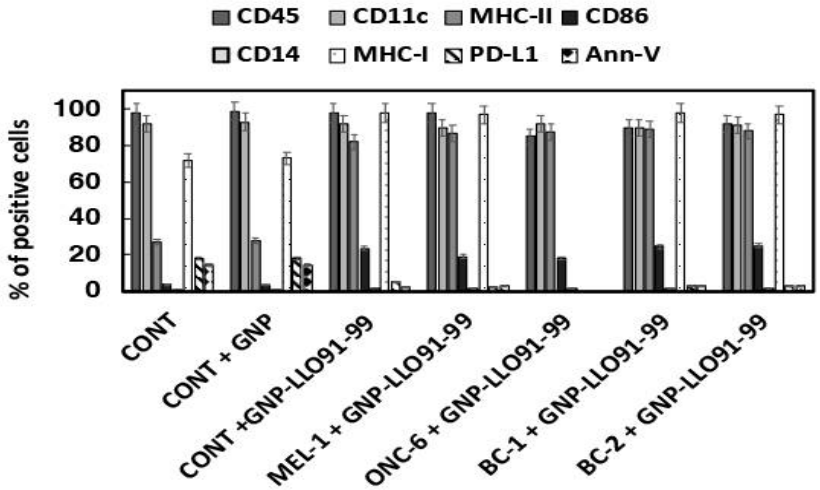

(a)

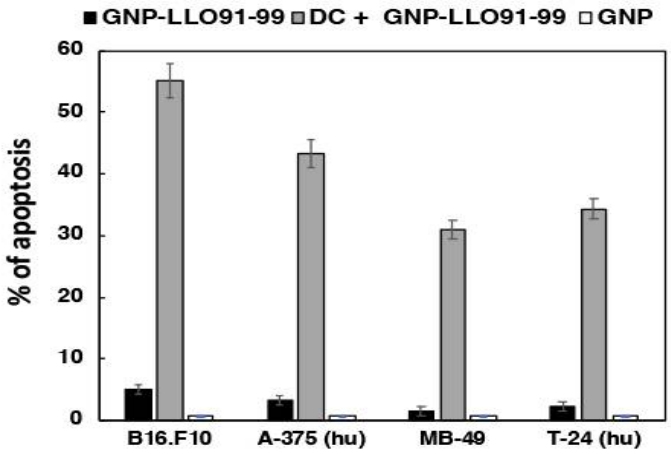

(b)

Figure 2. Adjuvant effects and immunogenic apoptosis abilities of GNP-LLO$_{91–99}$ nanovaccines. (**a**) Ex vivo differentiated MoDCs from patients (melanoma: MEL-1, MEL-2, bladder cancer: BC-1, BC-2) or healthy donors (CONT) with the phenotype CD45^{+}CD11c^{+}CD14^{-} were incubated or not with GNP-LLO$_{91–99}$ nanovaccines (+GNP-LLO$_{91–99}$ bars). FACS was performed to analyze cell surface markers, and results are expressed as the mean percentages of positive cells ± SD ($p \leq 0.05$). (**b**) Murine B16.F10 and human A-375 melanoma, and murine MB-49 and human T-24 bladder tumors were incubated with GNP-LLO$_{91–99}$ for direct apoptosis (black bars) or $\frac{1}{2}$ supernatants of DCs/MoDCs pre-treated with GNP-LLO$_{91–99}$ nanovaccines for immunogenic apoptosis (gray bars). Apoptosis was examined by FACS using the DNA marker, 7-AAD (7-AAD-PE), and the apoptotic marker, annexin V (annexin V-APC). Experiments were performed at least three times. Results are expressed as percentages of apoptotic cells ± SD ($p \leq 0.05$).

3.3. GNP-LLO$_{91–99}$ Nanovaccines Induced Immunogenic Apoptosis in Bladder Tumors

Once we evaluated the possibility that GNP-LLO$_{91–99}$ nanovaccines served as efficient adjuvants, we examined their induction of tumor apoptosis. For this purpose, we used available tumor cell lines of melanoma (murine B16.F10 or human A-375 cell lines) or BC (murine MB-49 or human T-24 cell lines). We examined two types of apoptosis by FACS: direct apoptosis and immunogenic DC-mediated apoptosis. GNP-LLO$_{91–99}$ nanovaccines induced low percentages of direct apoptosis onto BC or melanoma tumor cell lines, barely 5% in murine B16.F10 melanoma (black bars in Figure 2b), and showed no cytotoxicity (Supplementary Figure S2). Assays of DC-mediated immunogenic apoptosis imply incubation of tumor cell lines with $\frac{1}{2}$ of the supernatants of DCs or MoDCs, pre-incubated with GNP-LLO$_{91–99}$ nanovaccines. GNP-LLO$_{91–99}$ nanovaccines induced high percentages (35–55%) of immunogenic apoptosis in melanoma and BC (gray bars in Figure 2b). GNP-LLO$_{91–99}$ induction of immunogenic apoptosis seemed effective for tumors with significant T cell infiltration such as melanoma, BC, NSCLC lung tumors (murine TC-21 or human A-549 cell lines), or glioblastoma (murine O627 or human RG-1 cell lines), while not in tumors with low T cell infiltration, such as in hepatocellular carcinoma (murine Hepa 1-6 cell lines) [12,13], ovary tumors (hamster CHO cell lines), or SV-40-induced tumors (murine IC-21 macrophage-like cell lines) (Supplementary Figure S2). We conclude that GNP-LLO$_{91–99}$ nanovaccine induction of DC-mediated immunogenic apoptosis appears to explain their anti-neoplastic abilities.

3.4. Mechanisms of Anti-Neoplastic Abilities of GNP-LLO$_{91–99}$ Nanovaccines in Mice Models of Melanoma and BC

To validate the anti-neoplastic abilities of GNP-LLO$_{91–99}$ nanovaccines for BC, we established subcutaneous (s.c.) transplants of murine bladder MB-49 and melanoma B16.F10 tumor cell lines (protocol for all the following experiments is shown in Figure 3a) for 14 days, showing a size of 400–500 m^3.

First, we performed experiments to examine the effects of a single dose of GNP-LLO$_{91–99}$ nanovaccines at different times, i.e., 7, 14, and 23 days post-treatment, and observed similar results (Table 2, files labeled as + GNP-LLO$_{91–99}$). Mice were intravenously (i.v.) inoculated in their tails with a single dose of GNP-LLO$_{91–99}$ nanovaccines (50 μg/mouse), and 7 days post-treatment, mice were sacrificed, and sera and tumors were collected to examine the effects of nanovaccines (Figure 3b). GNP-LLO$_{91–99}$ nanovaccines reduced 5-fold tumor volume of B16.F10 melanoma and 4.7-fold of MB-49 bladder cell lines (GNP-LLO$_{91–99}$ bars in Figure 3b). The sizes of control tumors were 10-fold larger than tumors at 7 days, and survival of mice was 60% and 80% reduced, respectively, presenting tumor ulcerations (Table 2, SR and U columns). To avoid unnecessary pain to mice, for further experiments, we established a protocol of 14 days transplantation and 7 days treatment with GNP-LLO$_{91–99}$ nanovaccines (Figure 3a). GNP-LLO$_{91–99}$ nanovaccines implemented the survival rates (Table 2, SR columns of files labeled as + GNP-LLO$_{91–99}$) and blocked tumor growth at all times tested (TV columns).

Second, we explored the immune mechanisms able to explain the anti-neoplastic abilities of GNP-LLO$_{91–99}$ nanovaccines in BC mouse models, analyzing the cytokines in mouse sera. We confirmed a Th2 cytokine versus a Th1 pattern in mice transplanted with bladder MB-49 cell lines (light gray bars in Figure 4a), similar to the pattern detected with melanoma B16.F10 [6,7] (white bars in Figure 4a). In this regard, we detected high levels of chemokines recruiting neutrophils such as KC/CXCL1, participating in MDSC and tumor progression such as MIP-2, and high levels of cytokines such as IL-6 and TNF-a cytokines, while low levels of pro-inflammatory Th1-Th17 cytokines such as IFN-γ, IL-2, and IL-17A (CONT-B16F10 and CONT-MB-49, white and light gray bars in Figure 4a). Therefore, systemic production of chemokines/cytokines in mice transplanted with bladder MB-49 cell lines suggested an immunosuppression status [33] similar to the levels of BC or melanoma patients (Supplementary Table S1).

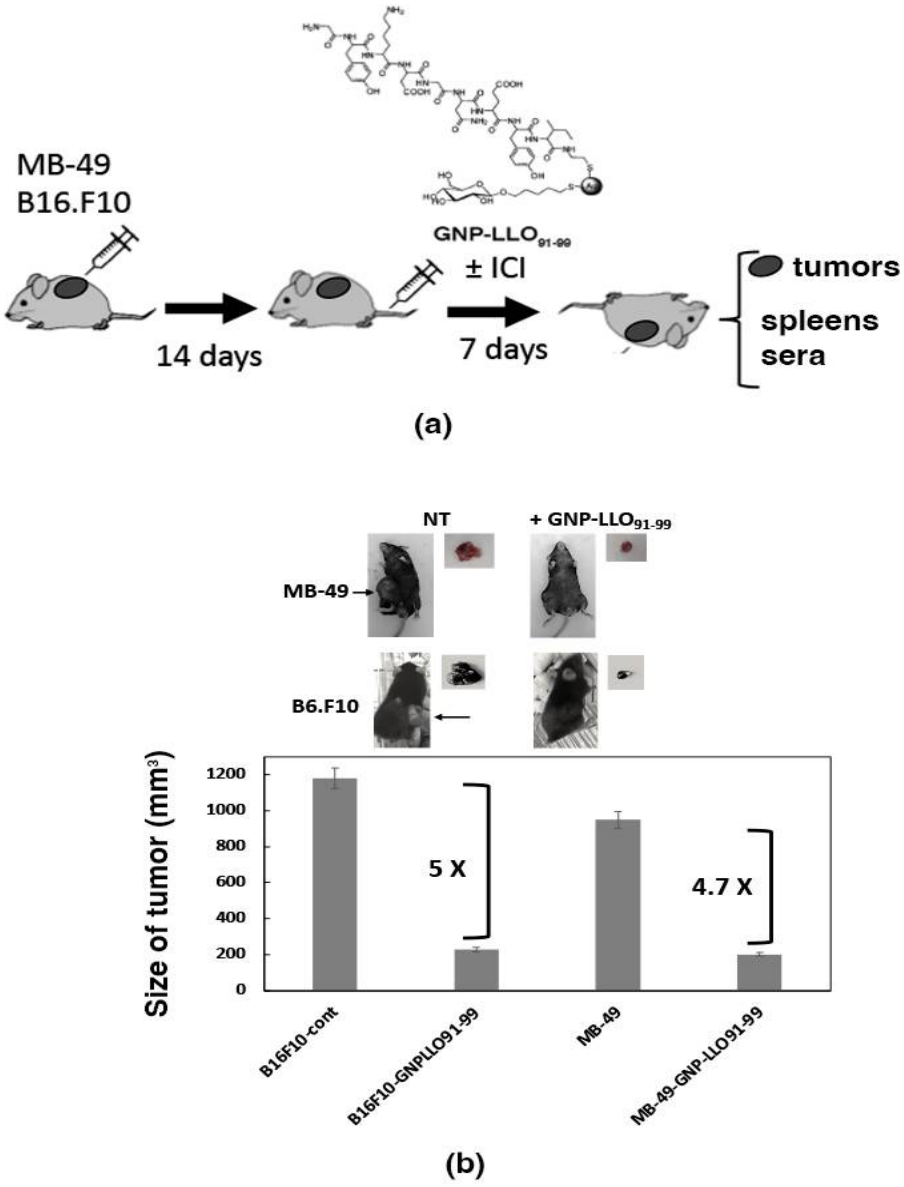

Figure 3. Anti-neoplastic abilities of GNP-$LLO_{91–99}$ nanovaccines. (**a**) General scheme of GNP-$LLO_{91–99}$ nanotherapy for all types of experiments. Melanoma (B16.F10) or BC (MB-49) tumor cell lines were s.c. transplanted into the right hind flanks of mice for 14 days. Next, mice were inoculated i.v. with a single dose of GNP-$LLO_{91–99}$ (50 μg/mouse) in the presence or absence of anti-CTLA-4 or anti-PD-1 antibodies (here labeled as ICI), or left untreated (CONT bars), and were sacrificed 7 days later. (**b**) GNP-$LLO_{91–99}$ treatment caused tumor reduction in B16.F10 melanoma and MB49 bladder tumor cell lines (upper images show the tumors isolated from mice, and lower graphs show the sizes measurements of isolated tumors).

However, innate immune responses were not identical in melanoma and BC, as we detected a high production of IL-17A cytokines in melanoma and normal levels in BC mice (CONT-B16F10 white bars versus CONT-MB-49 light gray bars Figure 4a). The treatment of transplanted mice with GNP-$LLO_{91–99}$ nanovaccines decreased the levels of Th2 cytokines KC, MIP-2, IL-6, and TNF-α and increased the levels of IFN-γ and IL-2, confirming the shift of Th2 to Th1 cytokine pattern in both mouse models of tumor transplantation, B16.F10 melanoma and MB49 bladder cell lines, suggesting a common action (black and dark gray bars in Figure 4a,b).

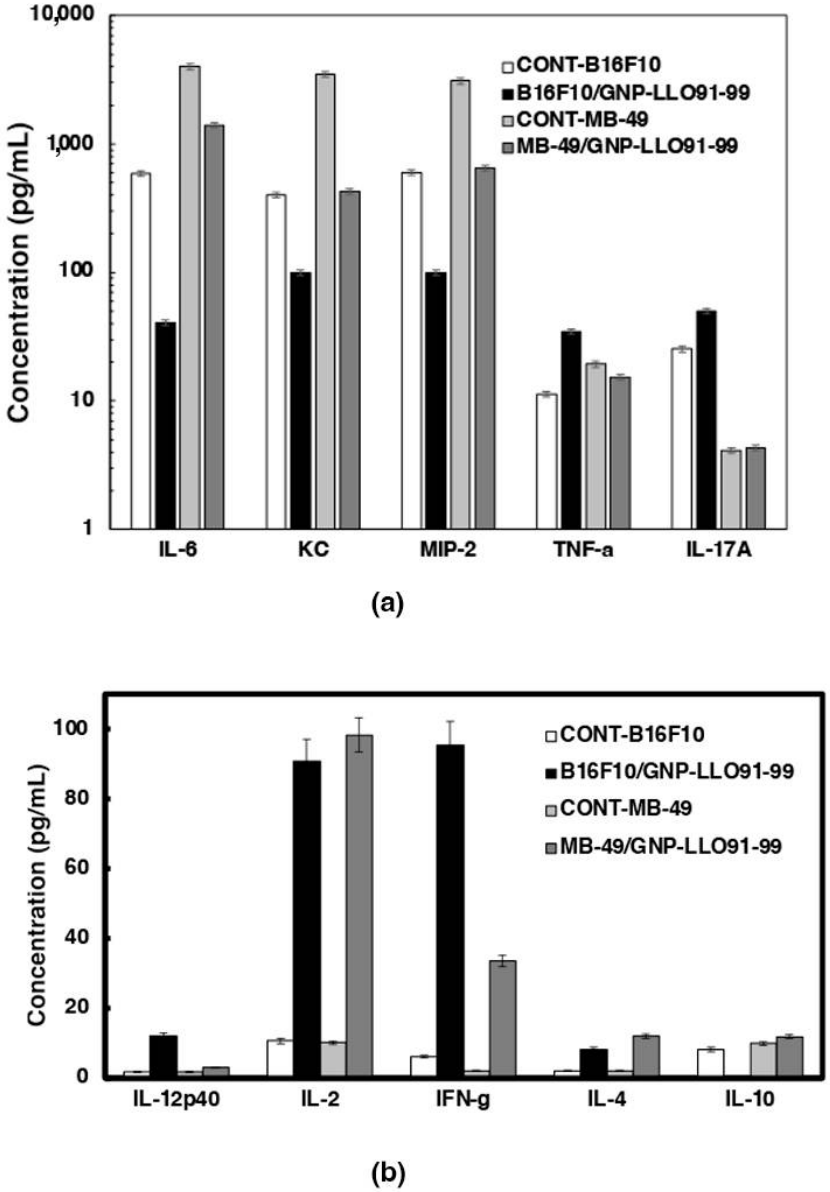

Figure 4. GNP-LLO$_{91–99}$ nanovaccines activate Th1 responses in mice models of melanoma and BC. Cytokines were measured in sera of mice transplanted with melanoma or BC and treated with GNP-LLO$_{91–99}$ nanovaccines (melanoma: white, BC: light gray bars) or untreated (melanoma: black, BC: dark gray bars) using a multiparametric Luminex kit (Milliplex MAP Mouse High Sensitivity T Cell Magnetic Bead Panel, EMD Millipore Corporation, Billerica MA) following the manufacturer's instructions. Cytokine concentrations are expressed as the average of three replicates in pg/mL ± SD. (**a**) Cytokines and chemokines produced by innate immune cells. (**b**) Cytokines produced by lymphocytes. Experiments were performed five times.

3.5. GNP-LLO$_{91–99}$ Nanovaccines Are Effective Immunotherapies That Blocked Immunosuppression

Next, we confirmed the immunosuppression status after isolation of tumor-infiltrated lymphocytes (TILs) of mice s.c. transplanted with melanoma or BC, and treated or not with GNP-LLO$_{91–99}$ nanovaccines. As shown in Figure 5a, BC basal status showed a higher immunosuppressive environment than melanoma, with higher levels of T_{reg} and MDSC ($Ly6G^+CD11b^+$) and lower levels of activated DCs ($CD11c^+$MHC-II^+) and macrophages ($F4/80^+$) (compare light gray versus white bars in Figure 4a).

Table 2. Clinical parameters of mice transplanted with melanoma and bladder tumors after GNP-$LLO_{91–99}$ therapy.

Tumor Cell Line and Treatment [a]	Day 7			Day 14			Day 23		
	SR [c]	U	TV [d]	SR	U	TV	SR	U	TV
MB49 + GNP-$LLO_{91–99}$ [b]	100% ± 1	-	426 ± 5	100% ± 1	-	436 ± 11	100% ± 1	-	490 ± 10
B16.F10 + GNP-$LLO_{91–99}$	100% ± 1	-	460 ± 2	100% ± 2	-	470 ± 13	100% ± 2	-	490 ± 9
MB49-NT	85% ± 2	-	1080 ± 5	45% ± 5	+/−	1680 ± 16	16% ± 2	+	4921 ± 19
B16.F10-NT	84% ± 2	-	1090 ± 6	42% ± 2	+/−	1690 ± 19	10% ± 2	+	5322 ± 20

[a] C57BL/6 female mice were s.c. transplanted with B16.F10 melanoma cells or MB49 bladder tumor cells (n = 10 mice/group) for 14 days showing a size of 400 m^3 for B16.F10 melanoma and 460 m^3 for MB49 bladder tumors. [b] Tumor transplanted mice received a single dose of GNP-$LLO_{91–99}$ i.v. (50 µg/mice) or saline (non-treated, NT) for 7 days. Number of surviving mice was counted at days 7, 14, or 23 post-transplantation. [c] Survival rates (SR) are expressed as the mean ± SD, and ulcerations (U) are indicated as positive (+) for abundant and severe ulcerations, (+/−) for rare and mild ulcerations, or negative (-) for absence of ulcerations. [d] Mice treated as in b were sacrificed, and tumors were recovered and measured with a caliper. Tumor volumes (TV) were calculated with the following formula: (length × $(width)^2$)/2. Results are the mean ± SD of tumor volumes. All experiments were repeated five times. Results are the mean ± SD ($p \leq 0.05$).

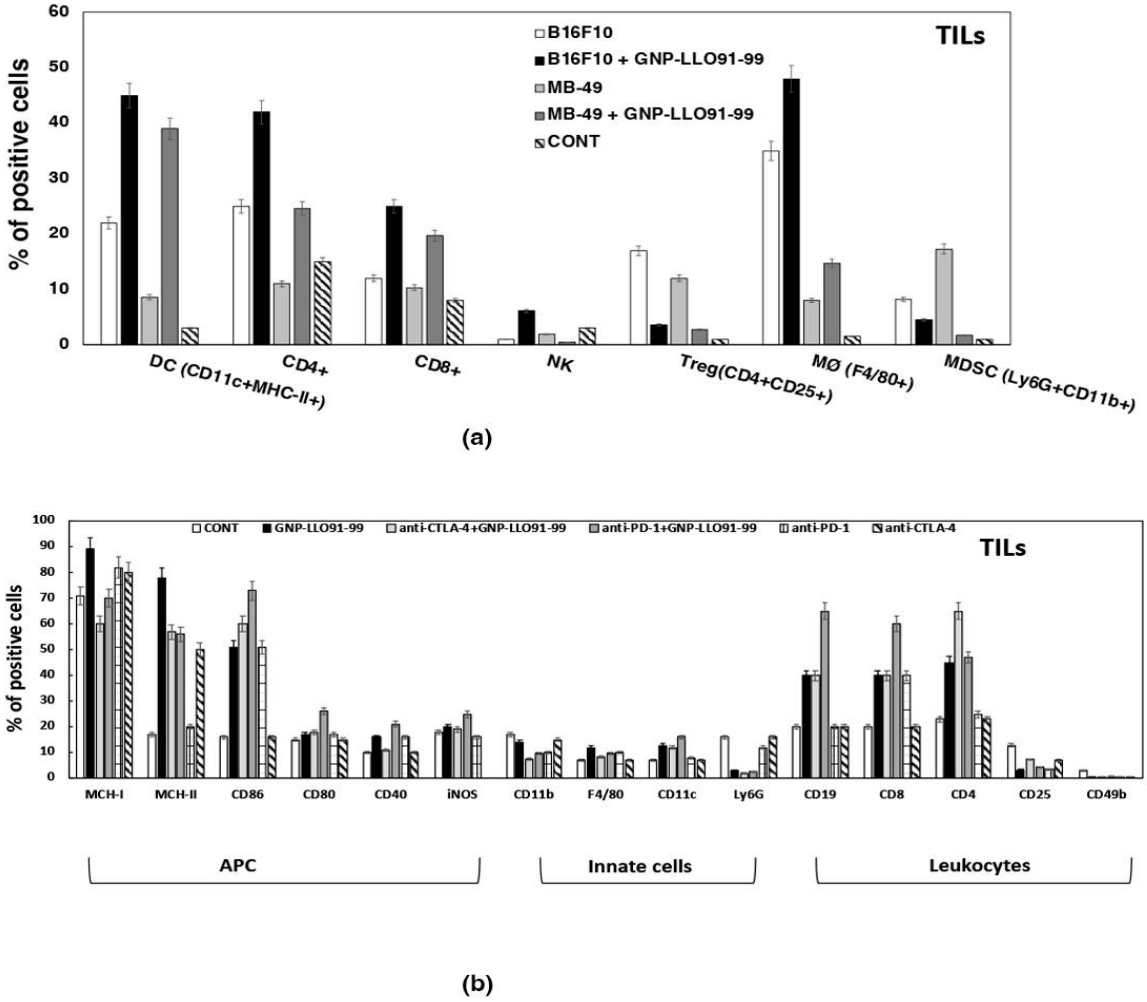

Figure 5. GNP-$LLO_{91–99}$ nanovaccines are effective immunotherapies in mice models of BC. (**a**) Mice s.c. transplanted with B16.F10 melanoma or MB-49 BC cell lines and treated or not with GNP-$LLO_{91–99}$ nanovaccines as in Figure 3 were sacrificed, tumors were collected, and TILs were isolated from interphases of Ficoll gradients (untreated mice: white bars for melanoma and light gray bars for

BC; GNP-LLO$_{91–99}$-treated mice: black bars for melanoma and dark gray bars for BC). FACS was performed to analyze cell surface markers and results are expressed as the mean percentages of positive cells ± SD ($p \leq 0.05$). (**b**) Mice s.c. transplanted with MB-49 bladder tumor cell lines and treated or not (CONT bars) with GNP-LLO$_{91–99}$, alone (black bars) or the combination of anti-CTLA-4 antibodies (light gray bars) or anti-PD-1 antibodies (dark gray bars). TILs were collected, and cell surface markers were analyzed by FACS. Results are expressed as the mean percentages of positive cells ± SD ($p \leq 0.05$).

GNP-LLO$_{91–99}$ nanovaccine action reduced immunosuppressed cells (T$_{reg}$, MDSC) in both tumor models and increased activated DCs and macrophages (compare black and dark gray bars in Figure 5a). Therefore, GNP-LLO$_{91–99}$ nanovaccines eliminated immune blockers in BC and melanoma, suggesting that they might function as immunotherapies for BC, as reported for melanoma [7].

Next, we verified that GNP-LLO$_{91–99}$ nanovaccines acted as immunotherapies in mice models of BC, exploring the immune populations in TILs of mice inoculated with a single dose of GNP-LLO$_{91–99}$ nanovaccines alone (50 µg/mouse) or in combination with anti-CTLA-4 (50 µg/mouse) or anti-PD-1 (50 µg/mouse) immunotherapies. GNP-LLO$_{91–99}$ nanovaccines, alone or in combination with anti-CTLA-4 or anti-PD-1 antibodies, increased the percentages of DCs with an activated MHC-II$^+$CD40$^+$CD86$^+$ phenotype of functional APC and the numbers of T and B cells (e.g., CD4$^+$, CD8$^{+,}$ and CD19$^+$ cells), while these treatments reduced the percentages of suppressor innate cells such as MDSC (Ly6G$^+$CD11b$^+$ granulocytes) and T$_{reg}$ (CD25$^+$ cells) (compare black, light gray, and dark gray bars in Figure 5b). We also included as controls mice treated with anti-CTLA-4 or anti-PD-1. As shown in Figure 5b, ICI alone cannot induce the percentages of activated DCs observed in GNP-LLO$_{91–99}$ nanovaccines combined with ICI. Anti-CTLA-4 treatment alone caused a moderate reduction in T$_{reg}$ but not as prominent as observed with GNP-LLO$_{91–99}$ nanovaccines combined with anti-CTLA-4.

In summary, GNP-LLO$_{91–99}$ nanovaccines appear to be valid immunotherapy for BC as well as melanoma. Moreover, the ability of GNP-LLO$_{91–99}$ nanovaccines to induce immunogenic apoptosis in solid tumors with high or low T cell infiltration, such as NSCLC lung cells or glioblastoma, and to activate MoDCs from patients with T cell-infiltrated solid tumors, such as prostate adenocarcinoma, multiform glioblastoma, or lung carcinoma, opens the possibility for future validation of GNP-LLO$_{91–99}$ nanovaccines as a neoadjuvant or immunotherapy for tumors with high or medium T cell infiltration.

4. Conclusions

GNP-LLO$_{91–99}$ nanovaccines appear to act as adjuvants for BC patients, as they promoted (i) the antigen presentation capacities of MoDCs of patients with BC (e.g., increasing the levels of MHC-I and MHC-II molecules as well as co-stimulatory CD86 molecules) and (ii) a Th1 cytokine pattern by releasing high levels of IL-12p70 and TNF-α with anti-neoplastic abilities.

In this study, GNP-LLO$_{91–99}$ nanovaccines presented anti-neoplastic abilities for BC, as they induced immunogenic apoptosis directed by dendritic cells and the cytokines released by them.

Moreover, GNP-LLO$_{91–99}$ nanovaccines showed immunotherapeutic abilities for BC, as they blocked the immunosuppression status of BC, increasing the numbers of cytotoxic T cells and DCs within the tumors and decreasing the number of immunosuppressive cells (T$_{reg}$, MDSC). In fact, GNP-LLO$_{91–99}$ nanovaccines adequately combine well and potentiate the action of ICI—both anti-CTLA-4 and anti-PD-1—supporting them as a novel nano-immunotherapy for BC.

5. Patents

F.R., S.Y.D. and C.A.D. participated as authors in the patent number WO2017144762 https://patentscope.wipo.int/search/es/detail.jsf?docId=WO2017144762 (accessed on 9 May 2022) and US20190045527 https://patentscope.wipo.int/search/es/detail.jsf?docId=

US237388381&_cid=P21-KC8ZLF-10597-1 (accessed on 9 May 2022), entitled to Instituto de Investigación Marqués de Valdecilla (IDIVAL).

Supplementary Materials: The following supporting information can be downloaded at: https://www.mdpi.com/article/10.3390/cancers14102413/s1, Figure S1: GNP-$LLO_{91–99}$ nanovaccines' effect as adjuvants of MoDCs of patients with different solid tumors; Figure S2: GNP-$LLO_{91–99}$ nanovaccines' effect on cell viability, and apoptosis of different solid tumors; Table S1: Cytokine patter in sera of patients with different solid tumors.

Author Contributions: C.A.-D., F.R. and I.D. designed and directed the experiments. A.Z., H.T.-N. and D.S.-C. performed all the experiments. H.T.-N. and A.Z. contributed equally to this study. M.M. designed the AuGNP coupled to $LLO_{91–99}$ peptide and performed all quality physical and chemical controls. N.M. provided counseling in the design of the nanomaterials and helped to design toxicity assays. Clinical physicians: M.D.-E., A.G.-C., F.C.-J., J.L.G.-B. and S.Y.-D. provided blood from melanoma, NSCLC, hepatocarcinoma, and glioblastoma patients, collected the informed consent of the patients; and helped with tumor mice models. E.G.-L. and J.G.O.-V. performed the cytokine measurements and analyses. All authors have read and agreed to the published version of the manuscript.

Funding: This research was funded by the CICYT program of the Ministry of Science and Innovation, grant number SAF2012-34203, co-funded in part by European FEDER funds "*A new way of making Europe*" and the COST European action ENOVA CA-16231; the Instituto de Salud Carlos III (ISCIII), grant numbers DTS18-00022 and PI19-01580 to C.A.-D.; the Bio-Health Research Program of Cantabria Government, grant number INNVAL17/01 to C.A.-D.; AstraZeneca private funds to I.D.; UNIR support to N.M. and C.A.-D.; and a predoctoral contract to D.S.-C. by the Bio-Health research program of the Cantabria government. M.M. thanks MIUR-Italy ("Progetto Dipartimenti di Eccellenza 2018–2022", allocated to Department of Chemistry "Ugo Schiff") and the COST European action INNOGLY CA-18103.

Institutional Review Board Statement: The study was conducted in accordance with the Declaration of Helsinki, under the Guide for the Care and Use of Laboratory Animals of the Spanish Ministry of Science, Research, and Innovation, and approved by the Institutional Review Board of the Committee of Clinical Ethics of Cantabria (CEm) entitled "Engineered nanovaccines with bacterial antigens for solid tumors immunotherapy", which included informed consent and general project information documents for patients (Acta number 03/2018. Internal code: 2018.007). The animal study protocol was approved by the Institutional Review Board of the Committee on the Ethics of Animal Experiments of the University of Cantabria (permit number: PI-01-17) and follows the Spanish legislation (RD 1201/2005). All surgeries were performed by cervical dislocation, and all efforts were made to minimize animal suffering.

Informed Consent Statement: Informed consent was obtained from all subjects involved in the study that could be revalued at any time by patients. Patients also received a document with the project information.

Data Availability Statement: The data presented in this study are available on request from the corresponding author.

Acknowledgments: We appreciate the critical comments of the MEDONLINE group at UNIR (Facultad de Ciencias de la Salud, Medical Center, UNIR, Madrid, Spain); the comments of previous members of the IDIVAL lab, such as R. Calderon-Gonzalez; and the gift of glioblastoma cells, O267, and RG-1 by J.L. Fernandez-Luna (Molecular Genetics Dept. HUMV, Santander, Spain). The LLO 91–99 peptide synthesis and purification of A. Paradela (Centro Nacional de Biotecnologia, CSIC, Madrid, Spain) are acknowledged. SciAnimation (https://sciani.com/portfolio/listeria-based-nanovaccines-novel-immunotherapies-solid-tumours/ accessed on 9 May 2022) is acknowledged for the preparation of graphical abstracts and videos.

Conflicts of Interest: The authors declare no conflict of interest. The funders had no role in the design of the study; in the collection, analyses, or interpretation of data; in the writing of the manuscript, or in the decision to publish the results.

References

1. Yao, Y.; Zhou, Y.; Liu, L.; Xu, Y.; Chen, Q.; Wang, Y.; Wu, S.; Deng, Y.; Zhang, J.; Shao, A. Nanoparticle-Based Drug Delivery in Cancer Therapy and Its Role in Overcoming Drug Resistance. *Front. Mol. Biosci.* **2020**, *7*, 193. [CrossRef]
2. Cheng, J.; Gu, Y.-J.; Cheng, S.H.; Wong, W.-T. Surface functionalized Gold Nanoparticles for Drug Delivery. *J. Biomed. Nanotechnol.* **2013**, *9*, 1362–1369. [CrossRef]
3. Marradi, M.; Chiodo, F.; García, I.; Penadés, S. Glyconanoparticles as multifunctional and multimodal carbohydrate systems. *Chem. Soc. Rev.* **2013**, *42*, 4728–4745. [CrossRef]
4. Calderon-Gonzalez, R.; Marradi, M.; Garcia, I.; Petrovsky, N.; Alvarez-Dominguez, C. Novel nanoparticle vaccines for listeriosis. *Hum. Vaccines Immunother.* **2015**, *11*, 2501–2503. [CrossRef]
5. Calderon-Gonzalez, R.; Terán-Navarro, H.; García, I.; Marradi, M.; Salcines-Cuevas, D.; Yañez-Diaz, S.; Solis-Angulo, A.; Frande-Cabanes, E.; Fariñas, M.C.; Garcia-Castaño, A.; et al. Gold glyconanoparticles coupled to listeriolysin O 91–99 peptide serve as adjuvant therapy against melanoma. *Nanoscale* **2017**, *9*, 10721. [CrossRef]
6. Calderon-Gonzalez1, R.; Bronchalo-Vicente, L.; Freire, J.; Frande-Cabanes, E.; Alaez-Alvarez, L.; Gomez-Roman, J.; Yañez-Diaz, S.; Alvarez-Dominguez, C. Exceptional anti-neoplastic activity of a dendritic-cell targeted vaccine loaded with a Listeria peptide proposed against metastatic melanoma. *Oncotarget* **2015**, *7*, 16855–16865. [CrossRef]
7. Terán-Navarro, H.; Calderon-Gonzalez, R.; Salcines-Cuevas, D.; García, I.; Marradi, M.; Freire, J.; Salmon, E.; Portillo-Gonzalez, M.; Frande-Cabanes, E.; García-Castaño, A.; et al. Preclinical development of Listeria-based nanovaccines as immunotherapies for solid tumors: Insights from melanoma. *Oncoimmunology* **2018**, *8*, e1541534.
8. Naran, K.; Nundalall, T.; Chetty, S.; Barth, S. Principles of Immunotherapy: Implications for Treatment Strategies in Cancer and Infectious Diseases. *Front. Microbiol.* **2018**, *9*, 3158. [CrossRef]
9. Hu, H.-G.; Li, Y.-M. Emerging Adjuvants for Cancer Immunotherapy. *Front. Chem.* **2020**, *8*, 601. [CrossRef]
10. Ribas, A.; Dummer, R.; Puzanov, I.; VanderWalde, A.; Andtbacka, R.H.I.; Michielin, O.; Olszanski, A.J.; Malvehy, J.; Cebon, J.; Fernandez, E.; et al. Oncolytic Virotherapy Promotes Intratumoral T Cell Infiltration and Improves Anti-PD-1 Immunotherapy. *Cell* **2017**, *170*, 1109–1119.e10. [CrossRef]
11. Sharma, P.; Hu-Lieskovan, S.; Wargo, J.A.; Ribas, A. Primary, Adaptive, and Acquired Resistance to Cancer Immunotherapy. *Cell* **2017**, *168*, 707–723. [CrossRef] [PubMed]
12. Yu, M.W.; Quail, D.F. Immunotherapy for Glioblastoma: Current Progress and Challenges. *Front. Immunol.* **2021**, *12*, 676301. [CrossRef] [PubMed]
13. Zhong, C.; Li, Y.; Yang, J.; Jin, S.; Chen, G.; Li, D.; Fan, X.; Lin, H. Immunotherapy for Hepatocellular Carcinoma: Current Limits and Prospects. *Front. Oncol.* **2021**, *11*, 589680. [CrossRef]
14. Alexandrov, L.; Nik-Zainal, S.; Wedge, D.; Aparicio, S.A.J.R.; Behjati, S.; Biankin, A.V.; Bignell, G.R.; Bolli, N.; Borg, A.; Børresen-Dale, A.; et al. Signatures of mutational processes in human cancer. *Nature* **2013**, *500*, 415–421. [CrossRef]
15. Klemm, F.; Maas, R.R.; Bowman, R.L.; Kornete, M.; Soukup, K.; Nassiri, S.; Brouland, J.-P.; Iacobuzio-Donahue, C.A.; Brennan, C.; Tabar, V.; et al. Interrogation of the Microenvironmental Landscape in Brain Tumors Reveals Disease-Specific Alterations of Immune Cells. *Cell* **2020**, *181*, 1643–1660.e17. [CrossRef]
16. Duan, Q.; Zhang, H.; Zheng, J.; Zhang, L. Turning Cold into Hot: Firing up the Tumor Microenvironment. *Trends Cancer* **2020**, *6*, 605–618. [CrossRef]
17. Joseph, M.; Enting, D. Immune Responses in Bladder Cancer-Role of Immune Cell Populations, Prognostic Factors and Therapeutic Implications. *Front. Oncol.* **2019**, *9*, 1270. [CrossRef]
18. De Liaño, G.A.; Duran, I. The continuing role of chemotherapy in the management of advanced urothelial cancer. *Ther. Adv. Urol.* **2018**, *10*, 455–480. [CrossRef] [PubMed]
19. Huang, P.; Ma, C.; Xu, P.; Guo, K.; Xu, A.; Liu, C. Efficacy of intravesical Bacillus Calmette-Guérin therapy against tumor immune escape in an orthotopic model of bladder cancer. *Exp. Ther. Med.* **2014**, *9*, 162–166. [CrossRef]
20. Noguera-Ortega, E.; Rabanal, R.M.; Gómez-Mora, E.; Cabrera, C.; Luquin, M.; Julián, E. Intravesical Mycobacterium brumae triggers both local and systemic immunotherapeutic responses against bladder cancer in mice. *Sci. Rep.* **2018**, *8*, 15102. [CrossRef]
21. Wood, L.M.; Guirnalda, P.D.; Seavey, M.M.; Paterson, Y. Cancer immunotherapy using Listeria monocytogenes and listerial virulence factors. *Immunol. Res.* **2008**, *42*, 233–245. [CrossRef] [PubMed]
22. Le, D.T.; Wang-Gillam, A.; Picozzi, V.; Greten, T.F.; Crocenzi, T.; Springett, G.; Morse, M.; Zeh, H.; Cohen, D.; Fine, R.L.; et al. Safety and survival with GVAX pancreas prime and Listeria monocytogenes-expressing mesothelin (CRS-207) boost vaccines for metastatic pancreatic cancer. *J. Clin. Oncol.* **2015**, *33*, 1325–1333. [CrossRef] [PubMed]
23. Sacco, J.J.; Evans, M.; Harrington, K.J.; Man, S.; Powell, N.; Shaw, R.J.; Jones, T.M. Systemic listeriosis following vaccination with the attenuated *Listeria monocytogenes* therapeutic vaccine, ADXS11-001. *Hum. Vaccines Immunother.* **2015**, *12*, 1085–1086. [CrossRef] [PubMed]
24. Hernández-Flores, K.G.; Vivanco-Cid, H. Biological Effects of Listeriolysin O: Implications for Vaccination. *BioMed Res. Int.* **2015**, *2015*, 360741. [CrossRef] [PubMed]
25. McDougal, C.; Sauer, J.-D. *Listeria monocytogenes*: The Impact of Cell Death on Infection and Immunity. *Pathogens* **2018**, *7*, 8. [CrossRef]

26. Maueröder, C.; Chaurio, R.A.; Dumych, T.; Podolska, M.; Lootsik, M.D.; Culemann, S.; Friedrich, R.P.; Bilyy, R.; Alexiou, C.; Schett, G.; et al. A blast without power-cell death induced by the tuberculosis-necrotizing toxin fails to elicit adequate immune responses. *Cell Death Differ.* **2016**, *23*, 1016–1025. [CrossRef]
27. Martínez-Ávila, O.; Hijazi, K.; Marradi, M.; Clavel, C.; Campion, C.; Kelly, C.; Penadés, S. Gold manno-glyconanoparticles: Multivalent systems to block HIV-1 gp120 binding to the lectin DC-SIGN. *Chem. Eur. J.* **2009**, *15*, 9874. [CrossRef]
28. Rodriguez-Del Rio, E.; Marradi, M.; Calderon-Gonzalez, R.; Frande-Cabanes, E.; Penades, S.; Petrovsky, N.; Alvarez-Dominguez, C. A gold glyco-nanoparticle carrying a listeriolysin O peptide and formulated with AdvaxTM delta inulin adjuvant induces robust T-cell protection against listeria infection. *Vaccine* **2015**, *33*, 1465. [CrossRef]
29. Zhou, M.; Zeng, C.; Chen, Y.; Zhao, S.; Sfeir, M.Y.; Zhu, M.; Jin, R. Evolution from the plasmon to exciton state in ligand-protected atomically precise gold nanoparticles. *Nat. Commun.* **2016**, *7*, 13240. [CrossRef]
30. Kuhn, S.; Hyde, E.J.; Yang, Y.; Rich, F.J.; Harper, J.L.; Kirman, J.R.; Ronchese, F. Increased numbers of monocyte-derived dendritic cells during successful tumour immunotherapy with immune-activating agents. *J. Immunol.* **2013**, *191*, 1984–1992. [CrossRef]
31. Shinde, P.; Fernandes, S.; Melinkeri, S.; Kale, V.; Limaye, L. Compromised functionality of monocyte-derived dendritic cells in multiple myeloma patients may limit their use in cancer immunotherapy. *Sci. Rep.* **2018**, *8*, 5705. [CrossRef] [PubMed]
32. Dmytryk, V.; Luhovska, T.; Yakovlev, P.; Savchuk, O.; Ostapchenko, L.; Halenova, T.; Raksha, N.; Tomchuk, V.; Vovk, T. Elevated levels of proinflammatory and anti-inflammatory cytokines in patients with bladder cancer depending on a tumor stage. *J. Biol. Res.* **2020**, *93*, 8632. [CrossRef]
33. John, B.A.; Said, N. Insights from animal models of bladder cancer: Recent advances, challenges, and opportunities. *Oncotarget* **2017**, *8*, 57766–57781. [CrossRef] [PubMed]